INTERNATIONAL JOURNAL FOR NUMERICAL METHODS IN ENGINEERING
Int. J. Numer. Meth. Engng 2004; **61**:238–254 (DOI: 10.1002/nme.1064)

Achieving minimum length scale in topology optimization using nodal design variables and projection functions

J. K. Guest[1], J. H. Prévost[1,*,†] and T. Belytschko[2]

[1]*Department of Civil and Environmental Engineering, Princeton University, Princeton, NJ 08544, U.S.A.*
[2]*Department of Mechanical Engineering, Northwestern University, Evanston, IL 60208, U.S.A.*

SUMMARY

A methodology for imposing a minimum length scale on structural members in discretized topology optimization problems is described. Nodal variables are implemented as the design variables and are projected onto element space to determine the element volume fractions that traditionally define topology. The projection is made via mesh independent functions that are based upon the minimum length scale. A simple linear projection scheme and a non-linear scheme using a regularized Heaviside step function to achieve nearly 0–1 solutions are examined. The new approach is demonstrated on the minimum compliance problem and the popular SIMP method is used to penalize the stiffness of intermediate volume fraction elements. Solutions are shown to meet user-defined length scale criterion without additional constraints, penalty functions or sensitivity filters. No instances of mesh dependence or checkerboard patterns have been observed.

KEY WORDS: topology optimization; length scale

1. INTRODUCTION

This paper offers a new approach to imposing a minimum length scale on structural members in discretized topology optimization problems. Nodal volume fractions are introduced as the new design variable and are projected onto element centroids to determine the traditional element-wise volume fractions ρ^e, or relative densities, that define topology.

The goal of topology optimization is to determine the layout of material of specified volume V in a domain Ω that maximizes the objective function for a given set of loads and boundary conditions. It is well-known that the continuum form of these problems is ill-posed, and thus

*Correspondence to: J. H. Prévost, Department of Civil and Environmental Engineering, Princeton University, Princeton, NJ 08544, U.S.A.
†E-mail: prevost@princeton.edu

Contract/grant sponsor: NASA University Research, Engineering and Technology Institute on Bio Inspired Materials (BIMat); contract/grant number: NCC-1-02037

Received 23 September 2003
Revised 5 January 2004
Accepted 23 January 2004

Published online 15 July 2004

generally lacks solutions. For the maximum stiffness problem, solutions can be improved by introducing more holes into the topology while keeping the total volume of material constant. This can lead to 'chattering' designs where the number of microscopic holes becomes unbounded [1]. The non-existence of solutions is reflected in the discretized version in the form of numerical instabilities. Although the discretized problem has solutions due to the finite number of elements, the solutions are influenced by the density of the mesh. As the mesh is refined, smaller holes can be introduced into the topology and members can become thinner. Another common problem is the occurrence of checkerboard patterns, or regions of alternating solid and void elements, in the final solution. Diaz and Sigmund [2] and Jog and Haber [3] showed that checkerboards are not optimal but rather result from numerical instabilities.

A significant amount of literature exists on preventing checkerboards patterns and mesh dependence. Checkerboards can be removed through smoothing or inhibited by using higher order finite elements [2, 3], non-conforming finite elements [4], or additional constraints [5]. A popular approach to eliminating mesh dependence is to restrict the design space so that a solution exists for the original continuum problem. One such restriction proposed by Ambrosio and Buttazzo [6] and first numerically implemented by Haber *et al.* [1] places a constraint on the total perimeter of the structure. Although it has been shown to yield mesh independent solutions, this global constraint does not prevent local thinning.

The design space can also be restricted by imposing a minimum length scale on members in the final topology. This yields mesh independent and checkerboard-free topologies as local features smaller than the physical length scale are prohibited. Petersson and Sigmund [7] used a local gradient constraint (or slope constraint) that limits the variation in ρ^e between adjacent elements. They reported similar results to those produced by Sigmund's heuristic filter which replaces the sensitivity of each element with a weighted average of neighbouring element sensitivities [8, 9]. These approaches produce mesh independent and checkerboard-free solutions, but also yield grey regions, i.e. regions containing intermediate volume fractions, along the boundary of the structure. The transition from solid to void (1 to 0) then occurs over several elements and some of these elements must be considered as solid for the minimum member size constraint to be satisfied. For a more detailed review of these procedures, the reader is referred to Reference [10]. More recently, Poulsen [11] suggested a constraint on the minimum length scale where violations are detected by passing a 'looking glass' over the design domain.

The approach introduced in this paper addresses the minimum length scale from a different perspective: the perspective of the nodes. We propose that nodal volume fractions be used as the design variable instead of element volume fractions. These nodal values are then projected onto the element centroids to determine the familiar element-wise volume fractions ρ^e that are used to determine the topology and consequently the stiffness and volume of material. Therefore, element volume fractions become a function of the nodal volume fractions.

This simple change coupled with an appropriate projection function appears to yield mesh independent and checkerboard-free solutions that meet the minimum member size criterion. These benefits are realized without additional constraints, penalty functions or filters.

Using nodal values as a design variable in topology optimization is not a new idea. Belytschko *et al.* [12] reported success using implicit functions to define the topology. The magnitude of the implicit function is determined at the nodes and then approximated elsewhere in the domain via shape functions. To solve the optimization problem, a regularized Heaviside step function and the extended finite element method are implemented. The approach presented here differs in

that it focuses on and provides direct control over length scale. It also uses the more traditional element-wise volume fraction variable ρ^{e} to define the topology.

The layout of the paper is as follows. Section 2 describes the projection scheme and introduces a linear projection function. The well-known minimum compliance problem is presented in Section 3 and is solved using the new approach in Section 4. Section 5 presents results for an example problem. A non-linear projection function is introduced and applied to example problems in Section 6 and conclusions are given in Section 7.

2. NODAL DESIGN VARIABLES AND THE PROJECTION SCHEME

Nodal volume fractions are the design variable in this method but do not carry much physical meaning on their own. They must be converted into element volume fractions before the topology, stiffness and volume of material can be determined. This conversion takes place through a projection scheme.

Many functions are available to project nodal values onto an element space—for example, the standard C^0 shape functions used in the finite element method. These shape functions, however, are by definition mesh dependent. Each node's shape function influences only the elements connected to that node. As the mesh is refined, the region of the domain it influences becomes smaller.

We require projection functions that are not influenced by mesh size. Instead, they should be based on a physical length scale that does not change with mesh refinement. The projection functions given here are constructed so that this parameter is equivalent to the minimum allowable radius $r_{\min}$ of members in the final topology. For this reason, the scale parameter is hereinafter referred to as $r_{\min}$.

Projecting nodal values onto an element requires two pieces of information: (i) the set of nodes included in the projection and (ii) the relationship between those nodes and the element volume fraction. The first issue is governed by the parameter $r_{\min}$. The second issue is more open—this paper offers two possibilities.

2.1. Identifying the nodes

The primary role of the scale parameter $r_{\min}$ in the projection scheme is to identify the nodes that influence the volume fraction of element e. Nodes are included in the element's projection function if they are located within a distance $r_{\min}$ of the centroid of e. This can be visualized by drawing a circle of radius $r_{\min}$ centred at the centroid of element e, thus generating the circular sub-domain Ω_w^e shown in Figure 1(a). Nodes located inside Ω_w^e contribute to the computation of ρ^{e}. It is worth repeating that $r_{\min}$ is a physical length scale, independent of the mesh. As the mesh is refined, $r_{\min}$ and consequently Ω_w^e do not change, as Figure 1(b) illustrates. The only difference between the two meshes is the number of nodes located inside Ω_w^e, and, therefore, included in the projection function. This is essential to generating mesh-independent solutions.

The search routine to identify the nodes lying inside each elemental Ω_w^e is expensive, particularly for fine meshes or large values of $r_{\min}$. However, it is performed only once at the beginning of the algorithm.

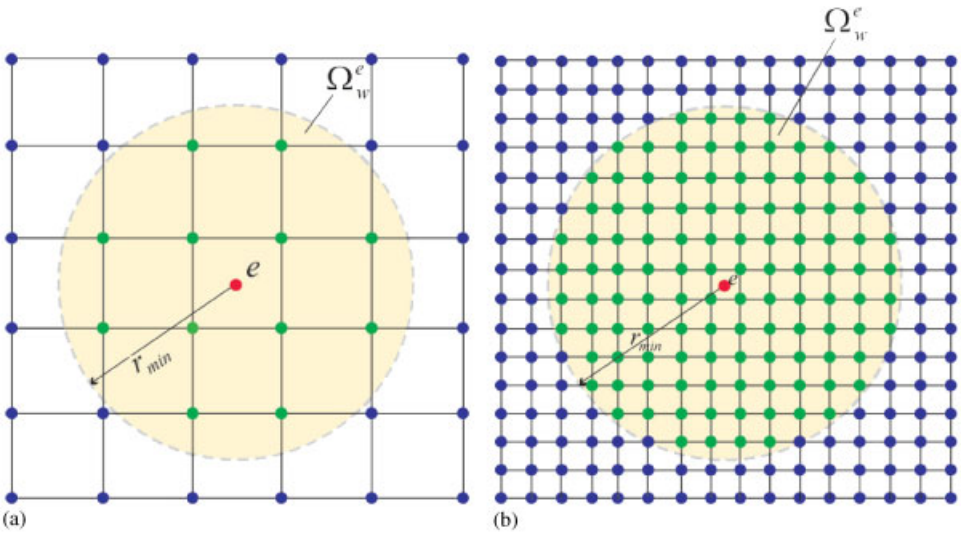

Figure 1. Nodes located inside the domain Ω_w^e are used in the projection scheme for element e—Ω_w^e does not change as mesh (a) is refined to (b).

2.2. A linear projection function

With the nodes identified, the second issue regarding the structure of the projection function can be addressed. This paper proposes two possible functions that ensure solutions meet the minimum length scale criterion. Let us first introduce the simpler linear projection function. A non-linear function that produces nearly 0–1 solutions is discussed in Section 6.

The linear projection function determines element volume fractions by performing a weighted average of the eligible nodal volume fractions. The weights assigned to the nodal volume fractions are based on proximity and determined by placing a weight function $w(\mathbf{x})$ at the centroid of element e, $\overline{\mathbf{x}}^e$. This weight function has a magnitude of 1 at the element centroid and decreases linearly to 0 over a distance $r_{\min}$ in all directions, essentially creating a cone of unit height and base $2r_{\min}$ as shown in Figure 2. To be more precise, the weight function of element e has a compact support Ω_w^e given by

$$\mathbf{x} \in \Omega_w^e \quad \text{if } r \equiv \|\mathbf{x} - \overline{\mathbf{x}}^e\| \leqslant r_{\min} \tag{1}$$

The linear weight function is defined by

$$w(\mathbf{x} - \overline{\mathbf{x}}^e) = \left\{ \begin{array}{ll} \dfrac{r_{\min} - r}{r_{\min}} & \text{if } \mathbf{x} \in \Omega_w^e \\ 0 & \text{otherwise} \end{array} \right\} \tag{2}$$

The weight function is independent of the mesh. If the mesh is refined, the only change will be an increase in the number of locations at which the function is to be evaluated.

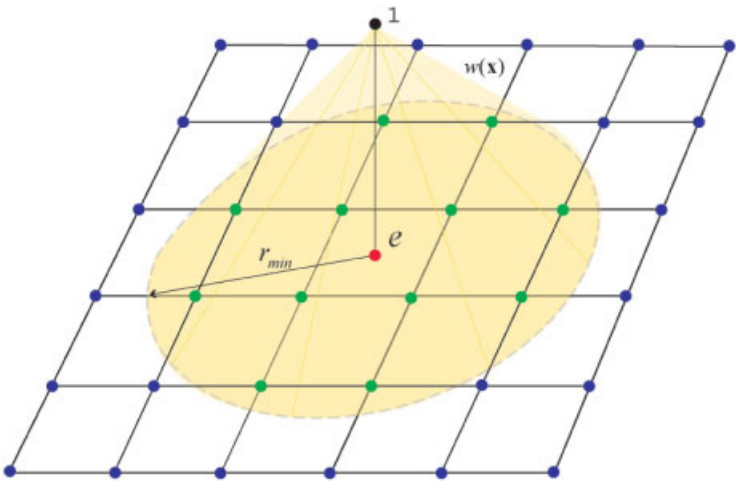

Figure 2. The weight function $w(\mathbf{x})$ for the linear projection scheme.

Let the element volume fraction of element e be denoted by ρ^{e}. We define an auxiliary set of nodal variables ρ_j that are related to the element volume fractions by

$$\rho^{\mathrm{e}} = \frac{\sum_{j \in S_e} \rho_j w(\mathbf{x}_j - \overline{\mathbf{x}}^e)}{\sum_{j \in S_e} w(\mathbf{x}_j - \overline{\mathbf{x}}^e)} \tag{3}$$

where S_e is the set of nodes in the domain of influence of element e (Ω_w^e) and $\mathbf{x}_j$ is the position of node j.

3. PROBLEM DEFINITION

In order to demonstrate this new approach to structural optimization let us consider the standard minimum compliance (maximum stiffness) problem. The object is to find the layout of material (structure) of volume V in the domain Ω that minimizes the compliance for a given set of loads and boundary conditions. Ignoring body forces, compliance is defined as

$$C = \int_{\Gamma_t} \mathbf{t}^{\mathrm{T}} \mathbf{u} \, \mathrm{d}\Gamma \tag{4}$$

where $\mathbf{t}$ are the tractions applied to the boundary Γ_t and $\mathbf{u}$ are the displacements.

The domain Ω is discretized into a finite number of elements. The goal is then to determine whether each element is a solid ($\rho^{\mathrm{e}} = 1$) or void ($\rho^{\mathrm{e}} = 0$), where the void ratio ρ^{e} is the traditional design variable for topology optimization.

Due to the inherent difficulty of binary programming problems, the 0–1 constraint on ρ^{e} is relaxed so the problem becomes a material distribution problem [13, 14] similar to the variable sheet thickness problem [15]. Although permitted, elements with intermediate volume fractions (between 0 and 1) are undesirable and are thus penalized to limit their presence in the final

solution. We use the popular solid isotropic material with penalization method (SIMP) developed by Bendsøe [14, 16] for the penalization. SIMP sets element stiffness tensors proportional to $(\rho^{\mathrm{e}})^p$, where generally $p \geqslant 3$, thereby decreasing the stiffness of elements with intermediate ρ^{e}, making them uneconomical; also see References [17–19]. Alternatively, a penalty term such as $\sum_e \rho^{\mathrm{e}}(1-\rho^{\mathrm{e}})$ could be added to the objection function [20].

The optimization problem, with element volume fractions expressed as a function of the nodal volume fractions $\boldsymbol{\rho}_{\mathbf{n}}$, is stated as

$$\begin{aligned} \min_{\boldsymbol{\rho}_{\mathbf{n}},\mathbf{u}} \quad & \mathbf{f}^{\mathrm{T}}\mathbf{u} \\ \text{s.t.} \quad & \mathbf{K}(\boldsymbol{\rho}_{\mathbf{n}})\mathbf{u} = \mathbf{f} \\ & \sum_{e\in\Omega} \rho^{\mathrm{e}}(\boldsymbol{\rho}_{\mathbf{n}}) v^e \leqslant V \\ & \rho_n^{\min} \leqslant \rho_n \leqslant 1 \quad \forall n \in \Omega \end{aligned} \tag{5}$$

where

$$\begin{aligned} \mathbf{K}(\boldsymbol{\rho}_{\mathbf{n}}) &= \mathop{\mathrm{A}}_{e} \mathbf{k}^e(\boldsymbol{\rho}_{\mathbf{n}}) \\ \mathbf{k}^e(\boldsymbol{\rho}_{\mathbf{n}}) &= (\rho^{\mathrm{e}}(\boldsymbol{\rho}_{\mathbf{n}}))^p \mathbf{k}_0^e \end{aligned} \tag{6}$$

and $\mathbf{f}$ are the applied loads, $\mathbf{K}(\boldsymbol{\rho}_{\mathbf{n}})$ is the global stiffness matrix formed by the usual assembly (A) of the element stiffness matrices $\mathbf{k}^e$, $\mathbf{k}_0^e$ is the element stiffness matrix of a solid element, v^e is the volume of element e, and $\rho_n^{\min}$ is the minimum allowable nodal volume fraction. For the linear projection function, $\rho_n^{\min} = \rho_{\min}^e$, where $\rho_{\min}^e$ is the minimum allowable element volume fraction set equal to a small positive number to ensure non-singularity of the global stiffness matrix. For example, we have used $\rho_{\min}^e = 10^{-3}$.

The principle of minimum potential energy allows us to express the equilibrium constraint in the objective function, yielding the well-known max–min formulation:

$$\begin{aligned} \max_{\boldsymbol{\rho}_{\mathbf{n}}} \min_{\mathbf{u}} \quad & \left(\tfrac{1}{2}\mathbf{u}^{\mathrm{T}}\mathbf{K}(\boldsymbol{\rho}_{\mathbf{n}})\mathbf{u} - \mathbf{f}^{\mathrm{T}}\mathbf{u}\right) \\ \text{s.t.} \quad & \sum_{e\in\Omega} \rho^{\mathrm{e}}(\boldsymbol{\rho}_{\mathbf{n}}) v^e \leqslant V \\ & \rho_n^{\min} \leqslant \rho_n \leqslant 1 \quad \forall n \in \Omega \end{aligned} \tag{7}$$

4. SOLUTION PROCEDURE

Problem (7) is solved using fixed point iterations. Displacements for the current iteration are found by solving the inner optimization problem for the current set of element volume fractions, which corresponds to solving the equilibrium equation:

$$\mathbf{K}(\boldsymbol{\rho}_{\mathbf{n}})\mathbf{u} = \mathbf{f} \tag{8}$$

These displacements are then held constant and the outer optimization problem is solved to determine the new nodal volume fractions:

$$\begin{aligned} \min_{\boldsymbol{\rho}_\mathbf{n}} \quad & -\Pi(\boldsymbol{\rho}_\mathbf{n}) \\ \text{s.t.} \quad & \sum_{e\in\Omega} \rho^{\mathrm{e}}(\boldsymbol{\rho}_\mathbf{n}) v^e \leqslant V \\ & \rho_n^{\min} \leqslant \rho_n \leqslant 1 \quad \forall n \in \Omega \end{aligned} \tag{9}$$

where

$$\Pi(\boldsymbol{\rho}_\mathbf{n}) = \frac{1}{2} \sum_{e\in\Omega} (\rho^{\mathrm{e}}(\boldsymbol{\rho}_\mathbf{n}))^p \mathbf{u}^{e\mathrm{T}} \mathbf{k}_0^e \mathbf{u}^e - \mathbf{f}^{\mathrm{T}}\mathbf{u} \tag{10}$$

and $\mathbf{u}^e$ is the displacement vector for element e, the strain energy term in (7) has been replaced by the sum of elemental strain energies, and the maximization problem has been converted to minimization form.

We solve (9) using the method of moving asymptotes (MMA) developed by Svanberg [21, 22]. MMA minimizes sequential convex approximations of the original function and is known to be very efficient for structural optimization problems. Solving (9) requires the gradient of $\Pi(\boldsymbol{\rho}_\mathbf{n})$ with respect to ρ_n:

$$\frac{\partial \Pi}{\partial \rho_n} = \frac{1}{2} \sum_{e\in\Omega} p(\rho^{\mathrm{e}}(\boldsymbol{\rho}_\mathbf{n}))^{p-1} \mathbf{u}^{e\mathrm{T}} \mathbf{k}_0^e \mathbf{u}^e \frac{\partial \rho^{\mathrm{e}}}{\partial \rho_n} \tag{11}$$

The term $\partial\rho^{\mathrm{e}}/\partial\rho_n$ will only be non-zero for elements whose domain Ω_w^e contains node n, i.e. the elements that use node n in their projection function.

For the linear projection function used in this paper, $\partial\rho^{\mathrm{e}}/\partial\rho_n$ is

$$\frac{\partial \rho^{\mathrm{e}}}{\partial \rho_n} = \frac{w(\mathbf{x}_n - \overline{\mathbf{x}}^e)}{\sum_{j\in S_e} w(\mathbf{x}_j - \overline{\mathbf{x}}^e)} \tag{12}$$

The convex sub-problem is then solved using an interior point method, a very efficient optimization method for convex problems; see References [23, 24] for details on implementing the interior point method.

It is well-known that the non-convexity of the design problem often leads to locally optimal solutions, especially when intermediate volume fractions are heavily penalized from the outset. We therefore use the continuation method as described by Sigmund [7] to reduce the probability of converging to a local minimum. The optimization problem is first solved with the exponent p equal to 1. The exponent is then increased by 0.5 and the problem is solved again using the previous solution as the starting topology. This pattern is continued until the exponent reaches 5.

5. CANTILEVER BEAM EXAMPLE

The cantilever beam problem is shown in Figure 3 and treated here as dimensionless. The design domain Ω has a length L of 40, height H of 25 and unit width. The domain is fixed

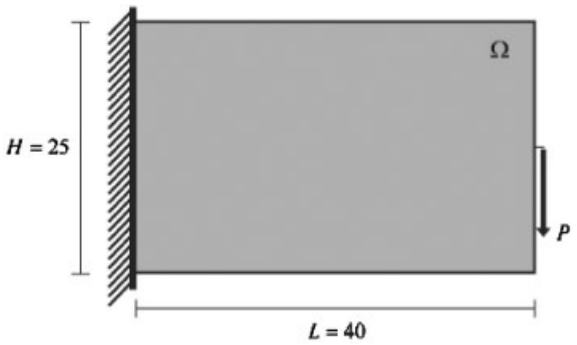

Figure 3. Cantilever beam problem.

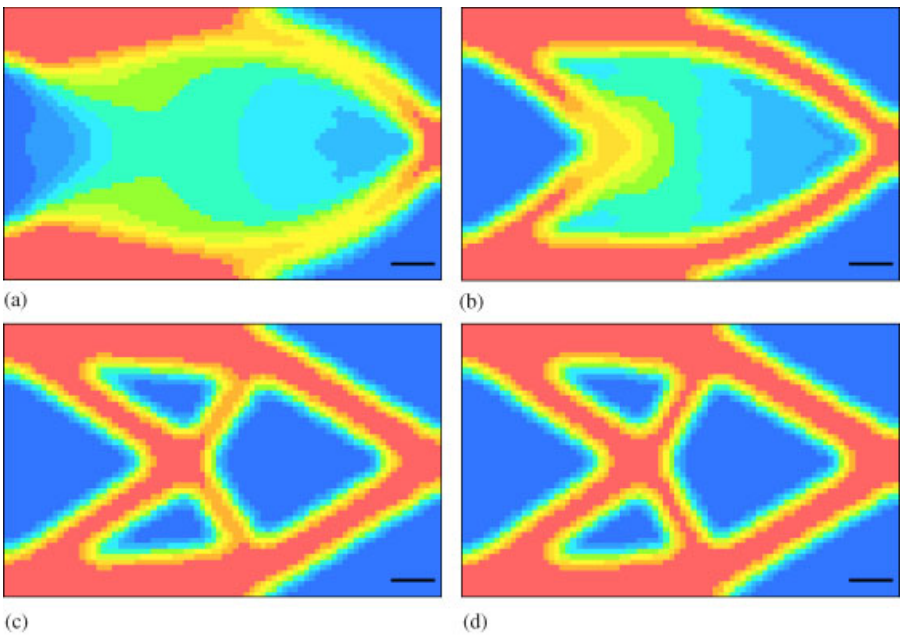

Figure 4. Design evolution during the continuation method: (a) $p = 1.0$; (b) $p = 1.5$; (c) $p = 2.0$; and (d) $p = 5.0$. The black bars represent the length $d_{\min} = 4$.

along the left edge and a point load $P = -1$ is applied midway up the free (right) end of the beam. Young's modulus is 10^6, Poisson's ratio is 0.25, and the allowable volume V of the structure is 50% of the domain volume, initially distributed uniformly. Minimum allowable member diameter $d_{\min}$ is 4 ($r_{\min} = 2$). The problem was solved using 4-node quadrilateral elements.

5.1. Design evolution

Figure 4 shows the converged topologies at various stages of the continuation method for an 80×50 element mesh ($h = \frac{1}{2}$, where h is the element size). As expected, the topology at

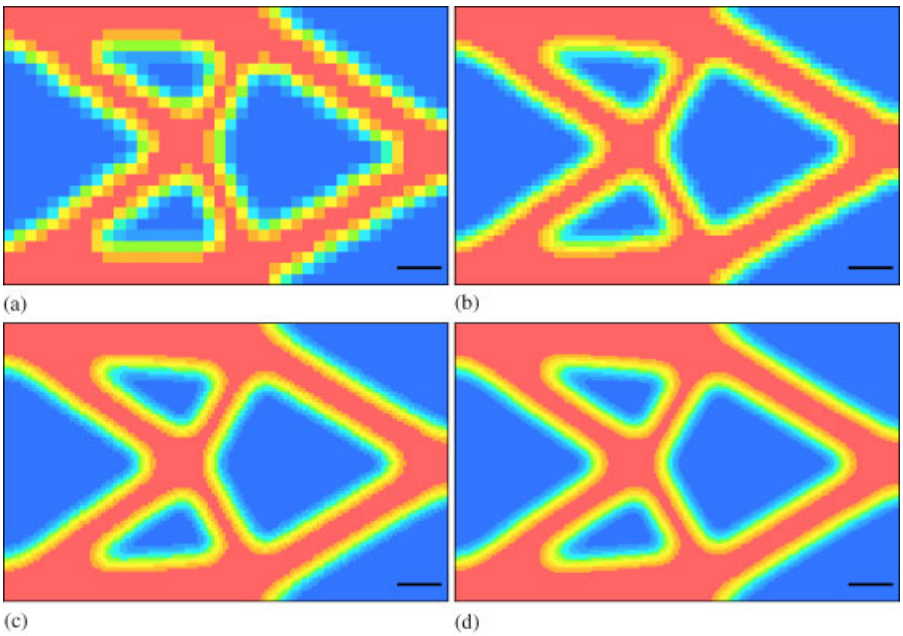

Figure 5. Optimal topology for different levels of mesh refinement when $d_{\min} = 4$: (a) 40×25 $(d/h = 4)$; (b) 80×50 $(d/h = 8)$; (c) 160×100 $(d/h = 16)$; and (d) 240×150 $(d/h = 24)$. The black bars represent the length $d_{\min}$.

$p = 1$ includes a significant number of elements with intermediate volume fractions. The outer boundaries of the structure, however, are well-defined. As the exponent increases, the number of elements with intermediate volume fractions decreases and the interior members develop. The general topology for this example is achieved by stage $p = 2$, and later continuation steps push more intermediate volume fraction elements to the bounds. The final solution ($p = 5$), shown in Figure 4(d) is consistent with solutions produced by Sigmund's sensitivity filter. Like those solutions and solutions obtained by slope constraints, Figure 4(d) contains grey regions. This shortcoming is discussed and corrected in Section 6.

The evolution of the topology is quite different from that reported by Belytschko *et al.* [12] with implicit functions. That approach allows the interior and exterior boundaries of the structure to form immediately as grey regions do not exist. The disadvantage is that the topology changes significantly during the iterative minimization due to the flatness of the objective function near the optimum.

5.2. *Mesh independence*

Figure 5 shows solutions for $r_{\min} = 2$ units using several mesh sizes. The figure demonstrates that the solution does not depend on the discretization: the only difference between the topologies is that the boundary of the structure becomes smoother with mesh refinement.

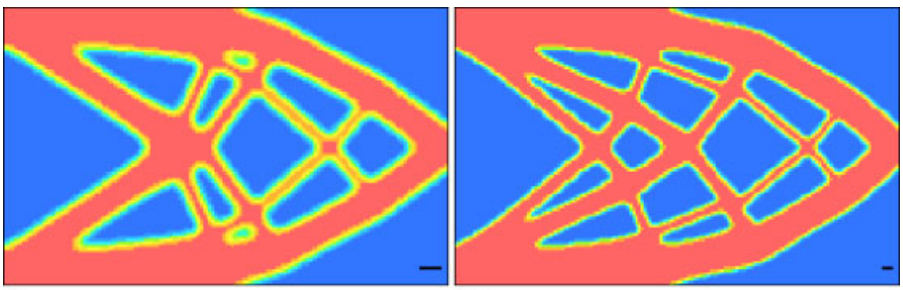

Figure 6. Optimal topologies using linear projection for various minimum allowable member diameters: (a) $d_{\min} = 2.0$; and (b) $d_{\min} = 1.0$, the black bars represent the length $d_{\min}$. Both cases use a 160×100 element mesh (d/h ratios of (a) 8 and (b) 4).

5.3. *Changing minimum member size*

The linear projection function provides direct control over member sizes through the scale parameter $r_{\min}$. The results in Figure 5 confirm this as all members have a thickness of at least 4 units. It should be noted, however, that some elements with intermediate volume fractions are used to satisfy this requirement. Thinner members can be allowed in the final topology by simply decreasing $r_{\min}$. Figure 6 shows topologies for minimum allowable member diameters of 2 and 1 unit. It is clear that decreasing $r_{\min}$ leads to finer structural members in the final topology. The 200×100 element mesh ($h = \frac{1}{4}$) used for Figure 6 is very fine but required to capture thinner structural members that are permitted when decreasing $r_{\min}$ to 0.5. The smallest allowable sub-domain Ω_w^e would include only the nodes comprising element e, and therefore $h < \sqrt{2} r_{\min}$. However, we have found that Ω_w^e should include nodes located outside of element e, therefore requiring $h < (\sqrt{10}/5) r_{\min}$ for a regular mesh.

6. OBTAINING 0–1 SOLUTIONS

A disadvantage of the linear projection function is the unavoidable fading effect that occurs along the edges of structural members. The transition from solid to void (1 to 0) occurs over several elements leaving intermediate volume fractions in the final topology. This appears to be a fundamental characteristic of linear projection schemes and cannot be prevented through penalization. This drawback is also observed in solutions obtained with slope-constraints and Sigmund's sensitivity filter. The boundary of the structure is usually interpreted as lying somewhere inside the grey region or some post-processing is performed to develop a clearer boundary.

6.1. *Non-linear projection functions*

The fading effect can be minimized or entirely prevented by a non-linear projection function. The Heaviside step function, for example, would insure a 0–1 boundary and maintain a minimum length scale when using the same nodes as the linear projection. Let us denote

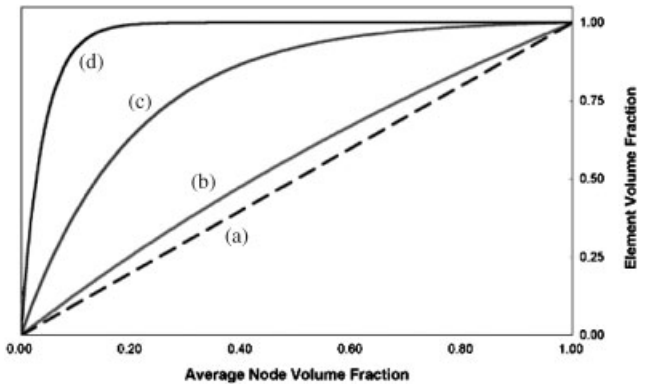

Figure 7. The regularized Heaviside step function for various magnitudes of β: (a) $\beta = 0$ (linear); (b) $\beta = 1$; (c) $\beta = 5$; and (d) $\beta = 25$.

the weighted average of nodal volume fractions within Ω_w^e as $\mu^e(\boldsymbol{\rho}_\mathbf{n})$. The weighted average function is repeated here for convenience:

$$\mu^e = \frac{\sum_{j \in S_e} \rho_j w(\mathbf{x}_j - \overline{\mathbf{x}}^e)}{\sum_{j \in S_e} w(\mathbf{x}_j - \overline{\mathbf{x}}^e)} \tag{13}$$

where $w(\mathbf{x})$ is the weighting function defined by (2).

The element volume fractions are now expressed as a Heaviside step function by

$$\rho^{\mathrm{e}} = \left\{ \begin{array}{ll} 1 & \text{if } \mu^e(\boldsymbol{\rho}_\mathbf{n}) > \rho_n^{\min} \\ \rho_{\min}^e & \text{if } \mu^e(\boldsymbol{\rho}_\mathbf{n}) = \rho_n^{\min} \end{array} \right\} \tag{14}$$

In other words, an element e is a void element if and only if all nodal volume fractions within Ω_w^e equal $\rho_n^{\min}$. On the other hand, a node with volume fraction greater than $\rho_n^{\min}$ yields a weighted average μ^e greater than $\rho_n^{\min}$ for all elements whose centroid lies within a distance $r_{\min}$ of that node. All of these elements are then solid elements, thereby satisfying the minimum length scale criterion.

In order to use the optimization algorithm outlined in Section 4, the Heaviside function must be regularized so that the gradient of ρ^{e} with respect to ρ_n is continuous. This can be achieved by the exponential function:

$$\rho^{\mathrm{e}} = 1 - \mathrm{e}^{-\beta \mu^e(\boldsymbol{\rho}_\mathbf{n})} + \zeta^e(\boldsymbol{\rho}_\mathbf{n}) \tag{15}$$

where the parameter β dictates the curvature of the regularization and $\zeta^e(\boldsymbol{\rho}_\mathbf{n})$ recovers the bounds on the element volume fractions:

$$\zeta^e = \mu^e(\boldsymbol{\rho}_\mathbf{n})\mathrm{e}^{-\beta} \tag{16}$$

The projection function (15) is linear when $\beta = 0$, and approaches the Heaviside step function as β approaches infinity. Figure 7 displays the regularization for a sample of β values.

The lower bound $\rho_n^{\min}$ must be adjusted for the selected β so that ρ^{e} achieves the lower bound (approximately) when Ω_w^e contains only nodes with minimum volume fractions—i.e. so that the following relationship holds:

$$\rho_{\min}^e \cong 1 - \mathrm{e}^{-\beta\rho_n^{\min}} + \rho_n^{\min}\mathrm{e}^{-\beta} \tag{17}$$

The third term is close to zero for most values of β and $\rho_{\min}^e$. Thus, the following estimation is often sufficient for $\rho_n^{\min}$:

$$\rho_n^{\min} = -\frac{1}{\beta}\ln(1 - \rho_{\min}^e) \tag{18}$$

It should be noted that (13), like the linear projection function, uses the weighted average of nodal values inside Ω_w^e to compute $\mu^e(\boldsymbol{\rho}_\mathbf{n})$. Alternatively, a standard mean could be used to determine the average nodal volume fraction. Although a standard mean may reduce the number of intermediate ρ^{e} in the final topology, preliminary results suggest the weighted average is more stable and produces smoother topologies.

We use the same optimization algorithm described in Section 4. The first derivative $\partial\rho^{\mathrm{e}}/\partial\rho_n$ given in (12) is replaced with

$$\frac{\partial\rho^{\mathrm{e}}}{\partial\rho_n} = \left(\beta\mathrm{e}^{-\beta\mu^e(\boldsymbol{\rho}_\mathbf{n})} + \mathrm{e}^{-\beta}\right)\frac{\partial\mu^e}{\partial\rho_n} \tag{19}$$

where

$$\frac{\partial\mu^e}{\partial\rho_n} = \frac{w(\mathbf{x}_n - \overline{\mathbf{x}}^e)}{\sum_{j\in S_e} w(\mathbf{x}_j - \overline{\mathbf{x}}^e)} \tag{20}$$

Problems are solved using the continuation method where the exponent penalty is raised gradually. We recommend starting with a low value of β, for example $\beta = 1$, to reduce the probability of oscillations and converging to a local minimum. If intermediate volume fractions exist in the converged topology, β and/or the exponent can be increased and the problem solved again until they are satisfactorily reduced.

6.2. Cantilever beam example

The cantilever beam problem is now solved using the non-linear projection function. For the results contained in this section, initial β is 1.0, and p and β were raised as described above.

The evolution of the topology is similar to the previously discussed evolution for the linear projection function. The converged solutions for the first continuation step ($p = 1$) are nearly identical as intermediate volume fractions are not yet penalized. Figure 8 contains the solution for $d_{\min} = 4$ units. The topology is similar to those created by the linear projection function but the number of intermediate volume fraction elements along the edges of structural members is greatly reduced.

As with the linear projection function, the non-linear function provides direct control over member sizes through $r_{\min}$. Figure 9 shows topologies for minimum allowable member diameters of 4, 2, 1.5 and 1. As $d_{\min}$ is reduced the problem becomes less restricted, thereby allowing thinner structural members to develop in the final topology.

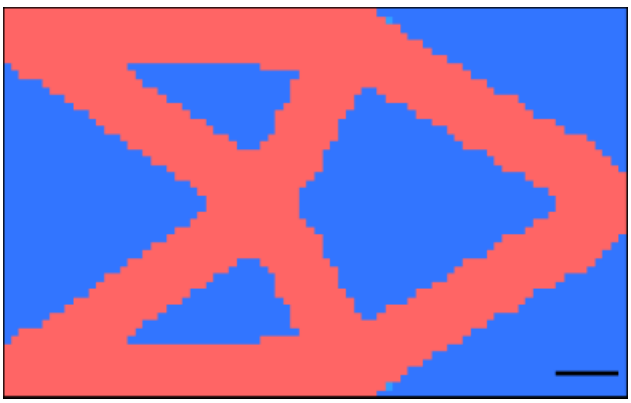

Figure 8. Optimal topology using the non-linear projection function for $d_{\min} = 4.0$—the black bar represents the length $d_{\min}$. Created using an 80×50 element mesh ($d/h = 8$).

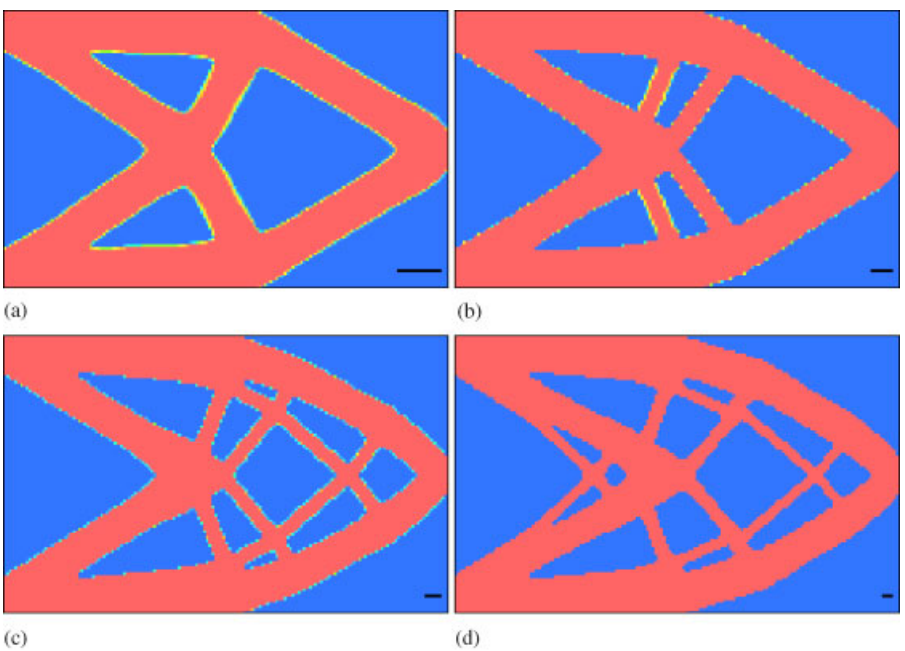

Figure 9. Optimal topologies using non-linear projection for various minimum allowable member diameters (represented by the black bars): (a) $d_{\min} = 4.0$; (b) $d_{\min} = 2.0$; (c) $d_{\min} = 1.5$; and (d) $d_{\min} = 1.0$. All cases use a 160×100 element mesh ($d/h =$ (a) 16; (b) 8; (c) 6; and (d) 4).

Comparing Figure 9 with the results obtained by the linear projection function (Figure 6) reveals that the reduction of intermediate volume fraction elements can lead to significant topological changes. A property of the linear function is that fading will occur, even with heavy penalization, and the minimum length scale is satisfied by the intermediate ρ^e in these regions.

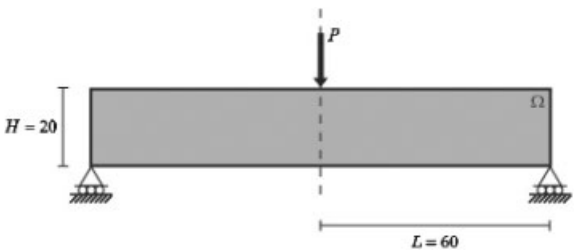

Figure 10. MBB-beam problem.

This allows for the formation of primarily 'grey members' (see Figure 6(a)). The non-linear function does not share this property as 0–1 solutions are obtainable. Under heavy penalization of intermediate volume fractions, members strive to satisfy the length scale criterion with only solid elements, thereby eliminating grey members from the final topology (see Figure 9(b)). This fundamental difference means the linear function can overestimate the intricacy of the topology if the end goal is a true 0–1 design.

Figure 9 also reveals that the non-linear projection yields fewer elements with intermediate volume fractions as the minimum length scale to mesh size ratio ($d_{\min}/h$) decreases. This trend is also seen in the next example. With a larger $d_{\min}$ (or smaller h) the number of nodes located inside of Ω_w^e increases, meaning the weight assigned to nodes with large ρ_n is extremely small for the elements at the edge of structural members. This leads to a lower nodal weighted average for that element and consequently a higher probability of becoming an intermediate volume fraction. Recall, however, that the mesh must be sufficiently refined as described in Section 5.3 to use the projection functions appropriately.

6.3. MBB-beam example

The second example is the so-called MBB-beam problem [25] and is shown in Figure 10. The problem is treated here as dimensionless and the deflection and stress constraints of [25] are relaxed. The design domain Ω has a length of 120 ($L = 60$), height H of 20 and unit width. Vertical displacement is restricted at the bottom corners of the beam and a point load $P = -1$ is applied at the midpoint on top of the beam. Due to symmetry only the right half of the beam is analysed. Young's modulus is 10^6, Poisson's ratio is 0.25, and V is 50% of the design domain volume, initially distributed uniformly. The problem was solved using 4-node quadrilateral elements.

Figure 11 displays the converged solutions for a minimum member diameter of 5 units when the linear and non-linear projection functions are implemented. The topologies are similar, with the non-linear function yielding almost no intermediate volume fraction elements in the final solution. Figure 12 contains the final topologies for various minimum allowable length scales. As $r_{\min}$ is reduced, the problem becomes less restricted and thinner members are permitted to develop.

Although not observed here, one potential shortcoming of this approach is that one-node hinges can exist in the final topology. Also referred to as point flexures, one-node hinges describe the event where two solid members are connected at only one node [26, 27]. This is similar to the checkerboard problem but is isolated to two elements. Consider two nodes,

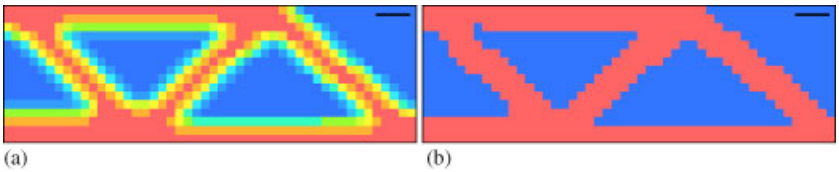

Figure 11. Optimal topologies for right half of beam produced by the: (a) linear; and (b) non-linear projection functions for $d_{\min} = 5.0$—the black bars represent the length $d_{\min}$. Both cases use a 48×16 element mesh ($d/h = 4$).

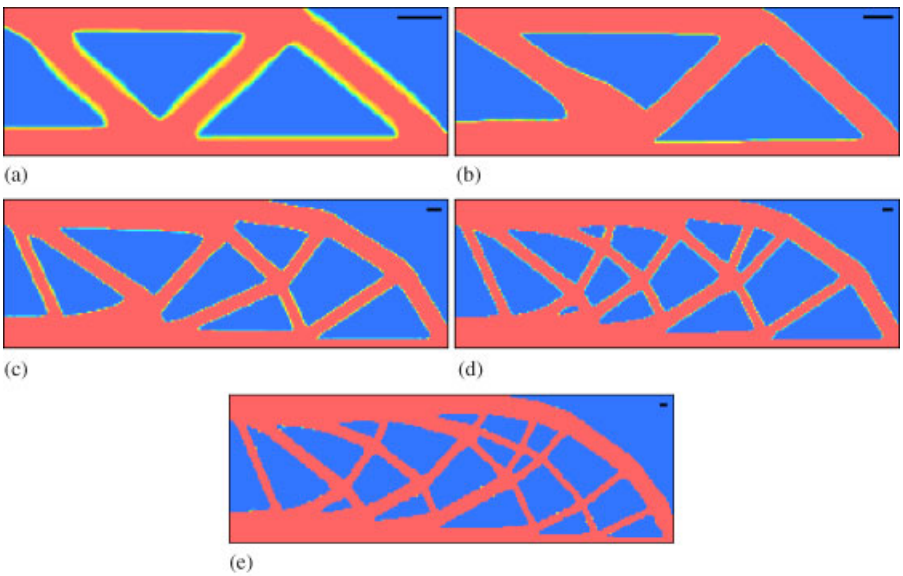

Figure 12. Optimal topologies using non-linear projection for various minimum allowable member diameters (represented by the black bars): (a) $d_{\min} = 6.0$; (b) $d_{\min} = 4.0$; (c) $d_{\min} = 2.0$; (d) $d_{\min} = 1.5$; and (e) $d_{\min} = 1.0$. All cases use a 240×80 element mesh ($d/h =$ (a) 24; (b) 16; (c) 8; (d) 6; and (e) 4).

separated by a distance $2r_{\min}$, that produce two circular solid members of radius $r_{\min}$. If all ρ_n between the nodes are minimum in magnitude, only the edges of the circular members will touch, potentially leading to one node hinges. This will not occur for the linear projection and has not been detected when the non-linear projection function features a weighted average of nodal values. However, one node hinges have been observed in topologies when both a standard mean and large β are used for the MBB beam problem.

7. CONCLUSIONS

The method presented in this paper offers direct control over the thickness of structural members in topology optimization problems. This is achieved through the use of mesh independent projection functions that convert nodal design variables into the familiar element-wise volume

fractions ρ^e. Despite this fundamental change, element volume fractions are still used to define the topology and therefore the stiffness, allowing for the use of Bendsøe's popular SIMP method to penalize intermediate volume fraction elements.

Preliminary results suggest that our methodology produces mesh independent, checkerboard-free and minimum member size compliant topologies. The simpler linear projection function appears to produce smooth solutions similar to those obtained by Sigmund's sensitivity filter. A byproduct of the linear function is the fading effect that, in some cases, is required to conform to minimum length scale. This can lead to 'grey members' and an overestimation of the intricacy of the topology as shown in the previous section. On the other hand, the non-linear projection function seems to produce nearly 0–1 topologies that satisfy the length scale criterion with solid elements. The minimum length scale is met without additional constraints, penalty functions or sensitivity filters. It should be noted that the non-linear projection function, in its present state, imposes a minimum length scale on only structural members, and does not directly impose a length scale on voids.

The approach has some similarities to the method presented in Belytschko *et al.* [12] which uses implicit functions to define the topology. Both methods use nodal values as the design variable and project those values onto element space. The projection functions here, however, ensure a minimum length scale as they are based on the physical length parameter $r_{\min}$. The projection in Reference [12] is local to the element as C^0 finite element shape functions are used. Advantages of the approach in Reference [12] are that 0–1 solutions are more readily obtained and solutions tend to be smoother for coarse meshes as implicit functions are used to define topology instead of element-wise volume fractions. A final similarity is that both methods regularize the Heaviside function to achieve 0–1 solutions. The regularization given in Equation (15) is just one possibility; other non-linear projection functions should be examined.

The methodology appears to be quite promising and is applicable to a wide-range of topology optimization problems. The only change in traditional problem formulations would be that element-wise volume fractions are expressed as a function of nodal volume fractions and these nodal values become the design variable.

ACKNOWLEDGEMENTS

This work is supported by the NASA University Research, Engineering and Technology Institute on Bio Inspired Materials (BIMat) under award No. NCC-1-02037. This support is gratefully acknowledged.

REFERENCES

1. Haber RB, Jog CS, Bendsøe MP. A new approach to variable-topology shape design using a constraint on perimeter. *Structural Optimization* 1996; **11**:1–12.
2. Diaz AR, Sigmund O. Checkerboard patterns in layout optimization. *Structural Optimization* 1995; **10**: 40–45.
3. Jog CS, Haber RB. Stability of finite element models for distributed-parameter optimization and topology design. *Computer Methods in Applied Mechanics and Engineering* 1996; **130**:203–226.
4. Jang G, Jeong JH, Kim YY, Sheen D, Park C, Kim M. Checkerboard-free topology optimization using non-conforming finite elements. *International Journal for Numerical Methods in Engineering* 2003; **57**: 1717–1735.
5. Poulsen TA. A simple scheme to prevent checkerboard patterns and one-node connected hinges in topology optimization. *Structural and Multidisciplinary Optimization* 2002; **24**:396–399.

6. Ambrosio L, Buttazzo G. An optimal design problem with perimeter penalization. *Calculus of Variations and Partial Differential Equations* 1993; **1**:55–69.
7. Petersson J, Sigmund O. Slope constrained topology optimization. *International Journal for Numerical Methods in Engineering* 1998; **41**:1417–1434.
8. Sigmund O. Design of material structures using topology optimization. *Ph.D. Thesis*, Department of Solid Mechanics, Technical University of Denmark, 1994.
9. Sigmund O. A 99 line topology optimization code written in Matlab. *Structural and Multidisciplinary Optimization* 2001; **21**:120–127.
10. Petersson J, Sigmund O. Numerical instabilities in topology optimization: a survey on procedures dealing with checkerboards, mesh-dependencies and local minima. *Structural Optimization* 1998; **16**:68–75.
11. Poulsen TA. A new scheme for imposing minimum length scale in topology optimization. *International Journal for Numerical Methods in Engineering* 2003; **57**:741–760.
12. Belytschko T, Xiao SP, Parimi C. Topology optimization with implicit functions and regularization. *International Journal for Numerical Methods in Engineering* 2003; **57**:1177–1196.
13. Bendsøe MP, Kikuchi N. Generating optimal topologies in structural design using homogenization method. *Computer Methods in Applied Mechanics and Engineering* 1988; **71**:197–224.
14. Bendsøe MP. *Optimization of Structural Topology*, *Shape*, *and Material*. Springer: Berlin, 1995.
15. Rossow MP, Taylor JE. A finite element method for the optimal design of variable thickness sheets. *AIAA Journal* 1973; **11**:1566–1569.
16. Bendsøe MP. Optimal shape design as a material distribution problem. *Structural Optimization* 1989; **1**: 193–202.
17. Zhou M, Rozvany GIN. The COC algorithm, part II: topological, geometry, and generalized shape optimization. *Computer Methods in Applied Mechanics and Engineering* 1991; **89**:197–224.
18. Mlejnek HP. Some aspects of the genesis of structures. *Structural Optimization* 1992; **5**:64–69.
19. Bendsøe MP, Sigmund O. Material interpolations in topology optimization. *Archive of Applied Mechanics* 1999; **69**:635–654.
20. Allaire G, Kohn RV. Topology optimization and optimal shape design using homogenization. In *Topology Design of Structures*, Bendsøe MP, Mota Soares CA (eds), Kluwer: Dordrecht, 1993; 207–218.
21. Svanberg K. The method of moving asymptotes—a new method for structural optimization. *International Journal for Numerical Methods in Engineering* 1987; **24**:359–373.
22. Svanberg K. A globally convergent version of MMA without linesearch. In *Proceedings of the First World Congress of Structural and Multidisciplinary Optimization*, Rozvany GIN, Olhoff N (eds), Goslar, Germany, 1995; 9–16.
23. Vanderbei RJ, Shanno DF. An interior-point algorithm for nonconvex nonlinear programming. *Computational Optimization and Applications* 1999; **13**:231–252.
24. Benson HY, Vanderbei RJ, Shanno DF. Interior-point methods for nonconvex nonlinear programming: filter methods and merit functions. *Technical Report*, Operations Research and Financial Engineering, Princeton University, 2001.
25. Olhoff N, Bendsoe MP, Rasmussen J. On CAD-integrated structural topology and design optimization. *Computer Methods in Applied Mechanics and Engineering* 1991; **89**:259–279.
26. Sigmund O. On the design of compliant mechanisms using topology optimization. *Mechanics of Structures and Machines* 1997; **25**:495–526.
27. Yin L, Ananthasuresh GK. A novel formulation for the design of distributed compliant mechanisms. *Proceedings of DETC '02*: *ASME 2002 Design Engineering Technical Conferences and Computers and Information in Engineering Conference*, Montreal, Canada, 2002.

